International Journal of
INTELLIGENT SYSTEMS AND APPLICATIONS IN ENGINEERING
ISSN:2147-6799 www.ijisae.org Original Research Paper

Enhancing Signal Processing Measurement for Pulse Rate Variability by Novel Algorithm and Regression Technique

[1]Saravanan Velusamy, [2]Pallikonda Rajasekaran Murugan, [3] Dr. G. Vishnuvarthanan, [4]Arunprasath Thiyagarajan, [5] Kottaimalai Ramaraj, [6]Vidyavathi Kamalakkannan

Submitted: 28/11/2023 **Revised**: 08/01/2024 **Accepted**: 18/01/2024

Abstract: The researchers looked into the relationship connected with magnetic element and sunlight, further the overall duration & delays of parasympathetic nervous method reactions to variation in sunlight and magnetic activity. Heart Rate Variability (HRV) measures were connected with sunlight and magnetic parameters utilizing a multi-element linear regression model with Bonferroni correction of multi-comparison tests after removing the circadian impacts of both information.Changes in sunlight radiation intensity were linked to changes in Pulse rates, which we interpret as a physiologic reaction to stress. Solar radiation elevation, gravitational wave fluxes, and Schumann's resonance amplitude were related to higher parasympathetic and HRV activity.HRV spectrograms were calculated for every participant utilizing Short Term Fourier Transform (STFT). A P-shift unfiltered fractional frequency response filter has utilized here, which gets smoother at P0. The filter is intended to provide a configurable median threshold that is excellent for slow ECG action and worse for rapid excursions. From the signal generator standpoint, it has been demonstrated that the flexible Unified Write Filter (UWFR) methodology in this technique provides optimal information extraction. In such a typical ECG signal sequence, the approach is necessary to track the T-wave, P-wave, and QRS-complex durations.

Keywords: *Autonomous nervous system; Heart Rate Variability; ECG; Denoising; UWFR filtering*

1. Introduction

Several papers hasestablished that describe the wide variety of physiological, modifications that are linked to modifications through geomagnetic &sunlight activity. Magnetic field disruptions will be included in public weather report bulletins in several nations. HF of conflict, rebellions, the terrorist assaults occur frequently were all connected to the sunlight cycle and a geomagnetic field that results disruptions [1]. High sunlight activity has been linked to not only social unrest, but also intervals of best blossoming of humans, includingspurts clear for creativity and innovation on design, sciences, arts, and positive social modification [2], and also varying human performance only in financial markets [3]. Several researcheshave found that geomagnetic and sunlight influences have an impact on a wide range of attitudes for the person and illenessresults, the neurological and cardiac systems are the most visibly impacted; even so, in people & animals, the intricacies of the bioactivity still are unclear. [4].

During recent decades, HRV has seen a significant growth in research and therapeutic therapy methods [5].HRV could be measured using a variety of analytical techniques, a most prevalent of that are power spectral density &duration domain assessment.These time intervals between every set of heartbeats are measured initially in both approaches.Individual beats with various underlying physiological mechanisms and osculates in different frequency bands are separated by power spectrum assessment from the complicated HRV waveform [6].An region that is curved inside the particular connectivity of a spectrum is represented by the power spectral density values.HRV tests show both short & long term rhythms due to connections between sympathetic neural activity and other brain functions, BP, breathing, and the brain's higher modulation systems [7].

[1]Research Scholar,Department of ECE,Kalasalingam Academy of Research and Education
Krishnankoil, Tamilnadu, India
SaravananVelusamyphd@outlook.com
[2]Department of Electronics and Communication Engineering, Kalasalingam Academy of Researchand Education
Krishnankoil, Tamilnadu, India
m.p.raja@klu.ac.in
[3]Associate Professor,Data Science – Division School of Computing Science and Engineering
VIT Bhopal University, Kothrikalan, Sehore
Madhya Pradesh – 466114, India.
vishnuvarthanan@vitbhopal.ac.in
[4]Department of Biomedical Engineering,Kalasalingam Academy of Research, and Education
Krishnankoil, Tamilnadu, India
t.arunprasath@klu.ac.in
[5]Department of Electronics and Communication Engineering, Kalasalingam Academy of Research and Education Krishnankoil, Tamilnadu, India
r.kottaimalai@klu.ac.in
[6]Department of Electronics and Communication Engineering, Selvam College of Technology
Namakkal, Tamilnadu, India
vidyavathiece.2010@gmail.com

The High Frequency range corresponds to time-based rhythms ranging from 2.5 to 7 secs. The band represents sympathetic activity, which is predominantly associated with the breathing cycle [8]. Te Low Frequency range corresponds on beats and phases of modulation ranging from 7 to 25 sec.The LF band has been hypothesised to reflect compensatory activation in addition as bar receptor activation implicated in shortterm BP regulation in peripheral 24hrs HRV recording [9].A number of researchers has disputed this viewpoint, claiming that the LF band primarily represents barorefex activity but not sympathetic activity in resting situations [10].

Despite the fact that all 24hrs HRV measures indicating poor HRV is associated to anhigher risk of bad results, VLF is a band that has a greater connection compared to certain bands in terms of all-cause death [11].VLF rotation are created by the dual cardiac neural method inside the heart, and the amplitude and frequency of these beats are changed by efferent parasympathetic activity, according to new findings [12].As a major sentimental stressor or times of physical action, sympathetic activations may boost VLF engery, crossover into alowest part of a Lower Frequency band.Low VLF power has also been linked to arrhythmic mortality and high infammation, and it has been linked to testosterone deficiency [13].Total Enegryis a composite overall HRV bands, hence a gauge of overall HRV on the physiological origins, while being heavily influenced by VLF power [14].

Frequency assessment is frequently performed utilising fast Fourier Transform (FT) or auto - regressive modelling, which necessitates determining the best model order [15]. Additional ways include determining the local frequency components of quasistationary signal fragments using greater moment spectra and cumulants of the signal or utilizing the STFT [16]. A continuous wavelet transform returns the correlation coefficients between both the signal and the rescaled wavelet of finite duration and power [17], which is an alternative to STFT for examining nonstationary signals. Another common technique is Empirical Mode Decomposition (EMD), that also extracts oscillating elements with symmetric envelopes from a nonlinear and nonstationary signal and can be used to calculate instantaneous amplitudes & frequencies utilizing the Hilbert transform [18]. It was utilised to investigate the data transfer between IMFs [19] and to discover the HRV element linked with breathing, among many other things. EMD was also used to investigate the HF element of foetal HRV rebuilt from IMFs with frequencies greater then 0.3 Hz [20]. [21] also looked at foetal HRV, using the sum of the previous IMFs as a proxy for the VLF element. HHT was used by Echeverria et al. to derive IMFs from 5-minute long series obtained from PhysioNet dataset. Researchers were able to illustrate the frequency components of the IMFs in this fashion, however they overlapped with in region of VLF to HF.

EMD also was utilised to look into modifications in the HRV spectrum when atropine was given. [22] recommended that IFM evaluations be improved by sequentially adding them from fine to coarse & coarse to fine.Because of the mode blending that caused artificial variation, the researchers concluded that immediate frequencies and amplitudes calculated for HF and LF elements from normal sinus arrhythmia must be regarded with caution [23]. Similar findings were published in [24]. Another noteworthy attempt was to utilize EMD to online HRV assessment by extrapolating IMFs associated to LF and HF to establish immediate frequencies and powers, with 60 percent fewer delays than the STFT.

A potential connections among sunlight and magnetic elements, as well as the total duration or delays in sympathetic nervous response to the modifications in sunlight& geomagnetic activity, was investigated in this study by accumulating HRV information for 72 consecutive hrsevery week utilising ambulatory HRV recorders over a five month period.The goal was to look at how the group's ANS responded to variation in sunlight and geomagnetic background behavior over time as reflected in HRV [25].

Based on the available literature, it became determined to evaluate MBF, EMD, and STFT efficiency initially.HRV is a non-uniformly sampled total of a effects of multiple physiological processes governing HR which can be isolated in the frequency response, and these impacts are considered as elements of hypothetical continuous HRV [26].

2. Materials and Methods

Eighteen healthy female employees (nine nursing staff, seven housekeeping, and Five from research division) volunteered to take part in the research.Its average lifespan was 33 yrs, with a range of 25 to 50 years old.There were no known physical or mental health problems among the participants, and they were full-time workers.A recognized health condition or the use of any drugs known to impact autonomic performance were also ruled out.Every participant signed a consent form and was allowed to leave the research at any moment.Two of the individuals withdrew out of the research due to irritation in at ECG electrode placements.The study followed all necessary criteria and met all applicable requirements for experimentation morality, and it was decree of the Minister of Health Research.

The participants had weekly recordings ambulatory HRV with Bodyguard HRV recorders for 24–72 hrs (Firstbeat Technologies Ltd, Finland).An inter-beat-interval (IBI), which is the duration in msec between successive pulse rate, is calculated by sampling the Electrocardiogram at 1000Hz.Every week, IBI information was kept locally as in internal storage and then transferred to the FTP server.Over a 5 month time from April to the last of Aug 2012, participants were recorded once a week for 72hrs.The total of 960 HRV recordings lasting 24 hours were acquired.

HRV signals were derived from the ECG recordings, and HRV spectrograms was calculated for every participant utilizing STFT.Visual inspection visually was used to evaluate the spectrograms, and 3 of these (from Patients #5, 7, & 11) were chosen for the further assessment because they had the most evident indication of HF.This criteria of acceptable quality HF tracks is significant because the HF elements derived from HRV and recorded breathing are directly correlated indicators, therefore comparisons of a HF elements recovered from HRV with recorded respiration are necessary.In addition, owing to evident consequences of electrode detachment, the first 54 minutes of Patient #11 information were eliminated.

3. Measurement

The IBI, Overall Energy, a LF/HF ratio and LF & HF engery have been the measurements HRV employed in this investigation.DADiSP 6.5 was used to analyse every recordings HRV that was transferred from a FTP server to a Computer work place.Inter-beat durations of 30 percent or less of the average of the past 4 durations were considered artefacts and were eliminated from the assessment record.During an automatically editing method, every recordings were personally inspected and, if necessary, adjusted by an expert technician.The HRV Task Force set criteria for processing daily recordings, which were analyzed in 5 min intervals.Any five - minute section with more than 10percent of the IBIs missing or deleted during editing was eliminated from the evaluation.For match the resolution of an atmospheric sets of data, the results of a 5 min section was averaged in to the hourly rates.The timestamps for local HRV information were translated to UTC and synchronised with atmospheric sets of data [27].Before uploading tothe common site, the information acquisition architecture captures and timestampsall information utilizing GPS time-signals.At the rate of 130Hz, every magnetometer is continually sampled.Fig. 1 depicts the period domain information for surrounding information activities over a course of the investigation.

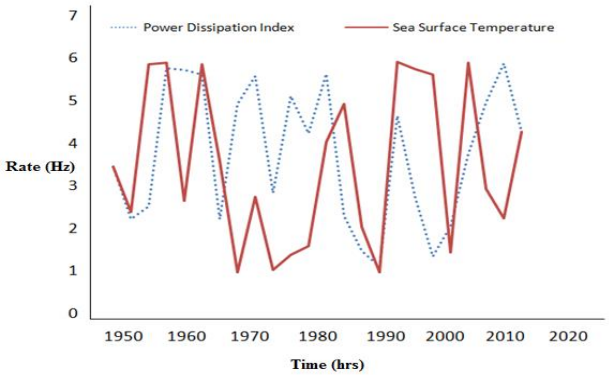

Fig 1 Activities of environmental information over the course of the investigation

On 14th July , there was a significant increase the indices as a consequence of theexpulsion of coronal volume which slam into the magnetic field of the earth at around 1800UT on the day.

3.1 Short-Time Fourier transform

Assumes signal local stationarity within a short-time sliding window, is among the most popular methods for frequency assessment of non-stationarity signals.The FFT is calculated from the samples at every window point, resulting in a local spectrum associated with a given time connectivity.Due to windowing, this discrete spectrum is simply an approximate of the true one, and it varies with the location of a window.A spectrogram is a time frequency chart made up of a series of such spectra placed one after another, with the energy capacity displayed on a colour scale.A widths of the evaluating windows were chosen to be equivalent to the duration of the lowest frequency in the respective range of HF, LF, & VLF, i.e. 6.5, 25 & 250s, respectively, because the searched elements have specified but varying frequency components.It was set to 30 mins at random for ULF. The windows was moved by one HRV2 sample, and the calculation outputs were allocated to temporal coordinates that corresponded to their centres.

There were numerous stages to the investigation. The Hann window was placed after the median was removed, and the signal was zero-padded to 2000 samples (providing a frequency resolution of 1 mHz) before the FFT was calculated.With a complicated spectrum $X_e(p)$, the spectral power density $C(h)$ for every frequency was calculated using the amplitude squared signal & Hann window lengths, as well as the windowing coefficient of power loss. Finally, the immediate amplitude was calculated using the following Equation 1.

$$X_e(p) = \sqrt{\sum_{h}^{u} C(h)} \qquad (1)$$

Where p is the position of a window midpoint, and u &h are the frequency range's boundaries.Similarly, the simultaneous stages were determined as the angles of $a_e(p)$, and their mean values$x_c(p)$in the provided frequency range was obtained.The magnitudes of the searching elements were calculated in Equation 2.

$$a_e(p) = x_c(p)\sin\big(\theta,(p)\big) \qquad (2)$$

3.2 Statistical Assessment

Multivariate linear regression was utilized to examine the information. As a single dependent element, every HRV element is examined. Each participant's set of data is managed separately in the initial assessment phase.To minimise the overall squared error of a linear system, regression coefficients were obtained for every HRV element and each individual set of data.The expected model is given in Equation 3:

Heart Rate Variable (HRV) = S_1F_1+ $S_2F_{2+\ldots.+}$ S_nF_n

HRV is the attached HRV element, F1, F2, and so on are are the independent surrounding elements, and S1, S2 and so on coefficient vectors. Hourly reports with missing information in any element was eliminated before the results obtained were produced, leaving only reflections with the complete group of surrounding measure. Furthermore, the information were adjusted to remove confounds circadian. The circadian normalisation has the side consequence of forcing both independent and dependent elements to have a zero overall median across the observation time, allowing the model of prediction to securely omit interrupt elements& calculate only slopes, as implied.

The R functions "lm" and "summarily" create a multiple dimensional coefficients of linear matrix with their accompanying conventional errors as a result of all these computations.Every of 6 HRV elements, as impacted by every of the 9 surroundingelements, has one regression coefficient in each of the 16 subjects at each of the 41 time delays. After computing the models, the following assessment stage were to calculate a cross contributorsmedian for the co - efficient of regression, effectively deleting a multiple dimensional array's participants dimension.Inside the conventional least-squares equation, this typical is the median of the membersregression co-efficients, separately weighted by their corresponding conventional errors:

$$\text{Mean} = \frac{\sum a_j/\mu_j{}^2}{\sum 1/\mu_j{}^2} \qquad (4)$$

where a_j are the specific evaluation, and $\mu_j$are the measurement associated paradoxes with those observations. The array for single participant evaluationcould be replacement by a single measurement, the weighted mean, within accompanying paradoxes assessment as a conclusion of this assessment. Figure 2 shows how time of sets can be utilized to investigate response time delays.

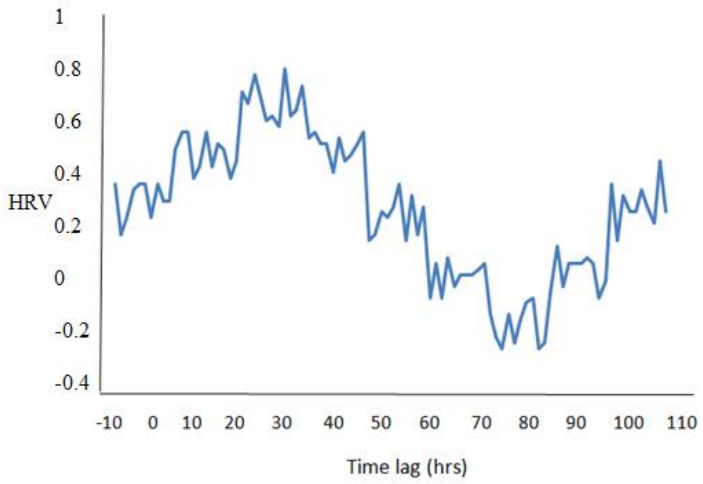

Fig 2: An atmospheric time series and an HRV time series

Te middle track depicts a same environmental information series following a 10-hour time shift. The HRV-environmental information correlations could be stronger in 10 delay than at 0 delay, denoting a physiological response to an external surrounding input that is delayed.

Last few values are solely relevant to inter operator variability, which is outside the scope of this study.Moreover, because it is immediately linked to the statistically significant of the given outcome and offers a scale independent solution metric of evaluating a contribution of various configuration file, the Z-score were employed extensively in both visualization and assessment of Z-scores. The above presumes that the mistakes are dispersed normally, but because of the computation explained is the medain of 16 independent cases calculated of the 16 members, any deviations from the norm would be very tiny, regardless of the dispersion of observational mistakes in a given way for a single member.

3.3 Corrections to Multiple Assessments

As a result of averaging the members contributions, the outcome is the multiple dimensional arrays of outcomes of 9 environmental elements, six HRV measurements, and 41 time delay, totaling 2214 analytic results. As assurance against making assessment mistakes by selecting relevant outcomes that seem purely by possibility, we used the correction Bonferroni for multiple assessments to this array of assessment outcomes, or to any subgroup which we may be examining in deeper level. The standard correction Bonferroni of the p-value of essential assessment by the overall number of assessment.In strict terms, and the suitable adjustment ofn studies within a p-value.

$$\rho_N{}^2 = \sum 1/\mu_j{}^2 \qquad (5)$$

$$C = Mean/\sigma_{Mean} \qquad (6)$$

$$Q_{correlation} = 1 - (1 - Q)^n \qquad (7)$$

$$Q_{correlation} = nQ - P(Q^2) \qquad (8)$$

$$Q_{correlation} = nQ \qquad (9)$$

may be demonstrated could be cautious, forever greater than areality p-value, with the minor mistake of P1. For this reason, the greatest single outcome in this whole study array has the p-value of 1.4×10^{-32}. As previously stated, the multiple-analyses modifications must take into account the fact that the identical regression techniques were used to evaluate 41 distinct time delays. When the Bonferroni adjustment 41test is applied to the delay outcomes for the one HRV to surrounding regression co-efficient, a most straight forward method of coping with multiple assessment problems is to allow for the fact that the actual relationship between geomagnetic surroundingelements and an HRV measure may engage an unidentified time delay.This enables a legitimate conclusion to be drawn about if that co-efficient has a statistically meaningful result for any of the tested time delays. This is commonly done informally in graphical depictions of the delay outcomes by showing the unaltered series of Z scores and setting a 5% envelope of relevance at ±3.24, the twotailed 5% threshold for the largest of 41 normal standard detracts.There are 54 similar coefficients in the assessment, which examines 6 HRV measures using 9 independent elements.Certain assessments, such as overall model relevance, necessitate applying a Bonferroni adjustment element of 54 to the most influential person outcomes.On the other category of assessment, Same as determining How personally of Spouse coefficients are individually significant at a given duration delay, do not necessitate a second Bonferroni adjustment above the one used for the number of delays.

3.4 Denoising Algorithm for ECG Signals

The UWFR smoothing method can be constructed for ECG signals specified if $M_{Minimum}$ and $M_{optional}$are present.The function smoothing UWFR is applied to distinct ECG signal segments with varying horizons in this approach.Operation smoothing UWFR over locations $P_{internal}$, $Q_{internal}$, Q, and P identifies of a ECG signal from Equations 10 - 14:

$$\tilde{a}_{m|m-q}(M)_1 = \tilde{a}_{m|m-q}\left(M_{optional}\right)(1: P_{internal} - 1), \qquad (10)$$

$$\tilde{a}_{m|m-q}(M)_2 = \tilde{a}_{m|m-q}\left(M_{optional}\right)(P_{internal}: P - 1), \qquad (11)$$

$$\tilde{a}_{m|m-q}(M)_3 = \tilde{a}_{m|m-q}(M_{Minimum})(P - Q), \qquad (12)$$

$$\tilde{a}_{m|m-q}(M)_4 = \tilde{a}_{m|m-q}\left(M_{optional}\right)(Q + 1: Q_{internal}), \qquad (13)$$

$$\tilde{a}_{m|m-q}(M)_5 = \tilde{a}_{m|m-q}\left(M_{optional}\right)(Q_{internal} + 1: R), \qquad (14)$$

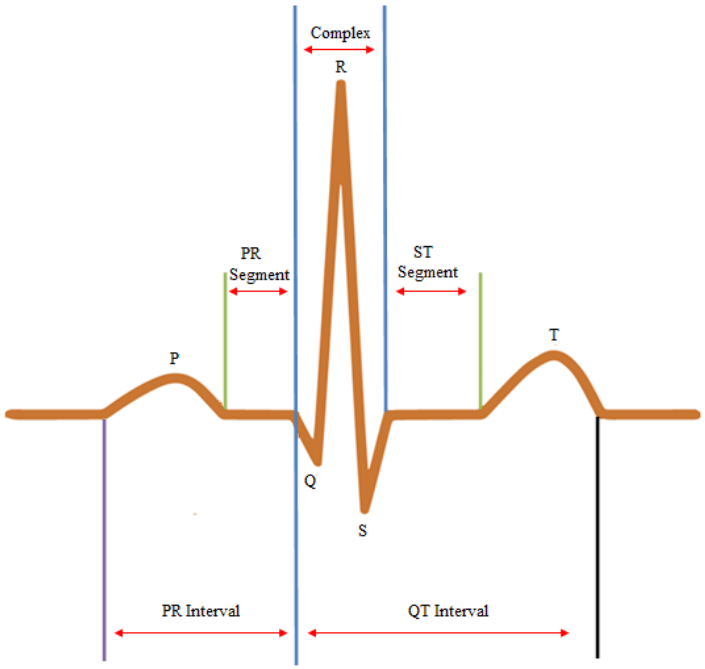

Fig 3: Measurement noise has tainted an actual single ECG beat

To apply $M_{optional}$, the 5th portions of Figure 3 are specified by (10) and (11), correspondingly.On [P, Q], an estimate that is equivalent to the original ECG signal without noise removal. To (12) and (13), the adaptive horizon $M_{optional}$ is used (14).With the one-time phase in the QRS complex area, n is reduced from $M_{optional}$. Beyond the QRS complex, n is steadily increased with a one time phase from $M_{Minimum}$to $M_{optional}$. Finally, at the fifth section, function calculates the ECG.

We create an calculation technique for ECG signal characteristics identification in this section, assuming that there is denoising via algorithm.To accomplish this, we first locate specific spots on the ECG cardiac pulse, after which we calculate appropriate amplitudes, timings, and angles. Unlike the techniques that have been devised.

Algorithm: Estimation of ECG

Input: $\tilde{a}_m$, I, $M_{Minimum,}M_{optional}$

Output: $\tilde{a}_{m|m-q}$

Step 1: ${\rho_N}^2 = \sum 1/{\mu_j}^2$

Step 2: for n from $M_{Minimum,}$to $M_{optional}$

Step 3: $\tilde{a}_{m|m-q}$ (n)=SmootUFIR($\tilde{a}_m$,n,I)

Step 4: $[Q_{internal}, P_{internal}, P, Q] = interQRS(\tilde{a}_m, interval)$

Step 5: $\tilde{a}_{m|m-q}(M)_1 = \tilde{a}_{m|m-q}(M_{optional})(1: P_{internal} - 1)$

Step 6: $\tilde{a}_{m|m-q}(M)_2 = \tilde{a}_{m|m-q}(M_{optional})(P_{internal}: P - 1)$

Step 7:$\tilde{a}_{m|m-q}(M)_3 = \tilde{a}_{m|m-q}(M_{Minimum})(P - Q)$

Step 8: $\tilde{a}_{m|m-q}(M)_4 = \tilde{a}_{m|m-q}(M_{optional})(Q + 1: Q_{internal})$

Step 9:$\tilde{a}_{m|m-q}(M)_5 = \tilde{a}_{m|m-q}(M_{optional})(Q_{internal} + 1: R)$

Step 10: $\tilde{a}_{m|m-q} = Concat((\tilde{a}_{m|m-q}(M)_1 + \tilde{a}_{m|m-q}(M)_2 + \tilde{a}_{m|m-q}(M)_3 + \tilde{a}_{m|m-q}(M)_4 + \tilde{a}_{m|m-q}(M)_5))$

4. Experimental Results

4.1 Dataset and Parameters

The Heart Rate Variability (HRV) of 16 individuals was measured for 72hrs each week and over a five - month time to assess Autonomic Nervous System (ANS) responses under normal underlying environment settings. The HRV waves were derived from the ECG recordings. Sunlight air velocity, KPindice, APindice, amount of sun-spots, as well as the geomagnetic polar capping indice all was taken into account in the assessment.

A visual examination was used to examine the spectrograms, and some of the patients with a more prominent trace of High Frequency (HF) were selected for additional assessment.

4.2 Results & Discussion

Tables 1 and 2 show the results of the environmental and HRV measure correlations.

Table 1: Correlations measure

Measurement of Correlations									
	1	**2**	**3**	**4**	**5**	**6**	**7**	**8**	**9**
1.	2	0.45	0.49	0.19	0.16	0.43	-0.23	0.25	0.46
2.	0.46	2	0.89	0.29	0.27	0.89	-0.29	0.16	0.59
3.	0.23	0.89	2	0.18	0.27	0.87	-0.23	0.16	0.23
4.	0.02	0.17	0.19	2	0.29	0.27	-0.19	0.12	0.16
5.	0.18	0.29	0.28	0.83	2	0.36	-0.36	0.28	0.19

Table 2. HRV measure correlations

Measurement of Correlations								
Variations	A	B	C	D	E	F	G	H
1.	2	0.8	0.9	0.83	0.82	0.7	0.78	-0.65
2.	0.65	2	0.75	0.76	0.75	0.79	0.83	-0.53
3.	0.79	0.7	2	0.8	0.95	0.83	0.97	-0.45
4.	0.68	0.78	0.89	2	0.98	0.95	0.93	-0.43
5.	0.83	0.81	0.95	0.87	2	0.89	0.87	-0.36

Sunlight wind speed were substantially connected to the Kp (r 0.50, $p < 0.01$) and Ap (r 0.35, $p < 0.01$) indices, ULF energy, and inversely connected with cosmic radiation numbers (r 0.15, $p < 0.01$), in agreement with earlier findings.The amount of suns-pots was similarly substantially associated with the sunlight radiation flux, as anticipated.The Schumann Resonance Energy was shown to be substantially associated with cosmic radiation counts, both positively and negatively. Kp, Ap and CP were all positively associated with ULF energy. The exception of High Frequency energy, where the connections to IBI, Total Energy, VLF energy was all larger than saw in single 24hrs recordings, the connections among the HRV elements were as anticipated and in agreement with earlier studies.

The outcomes of the multiple variate linear regression among surrounding and elements HRV indicated the variety for important results, with distinct Metrics for HRV reacting to changes in environmental parameters at varying time delays . In hours 12 through 15, IBIs was positively linked with variation in the amount of suns-pots. .At hour 10, and again from hours 12 to 15, there was a considerable increase in TP. From hour 10 to hour 15, HF was also favourably associated.The VLF was essentially same, although it did not become substantial until the 13th hour, so it stayed so until hour 15.The LF were not statistically significant.

In the IBIs, TP, VLF, and HF energy, there's an instantaneous, robust positive correlation response to sunlight radiation flux . For the first 2 hours, the IBI reaction was considerable.The TP energy reaction remained substantial for the first 8 hours, then for the 19th and 20th hours, and finally for the last 34 hours period of assessment.The VLF reaction was substantial for the first six hours, as well as during hours 35, 37, 38, and 39, whereas the HF reaction was substantial for the first 5 hours.At no point during the period of assessment did the LF or LF/HF ratios attain statistical significance.Over a 40-hour period, there was no correlation between sunlight wind speed and any of the HRV elements.

Connections for Schumann Resonance Power and ULF Energy are shown in Figure 4. A lot of significant associations were discovered.The IBIs were the first to react to the SRP, becoming substantial in the fourth hr and remaining substantial through hour 31, as well as in the 36 to 40th hour.During hrs 8 to 18, as well as hrs 21

to 37, the Total Power reaction were strong.From hrs 10 to 17, and then again from hrs 22 to 33, VLF energy were significant.Beginning at hr 9, LF energy increased steadily until hr 16, and then again around hrs 21 & 38.

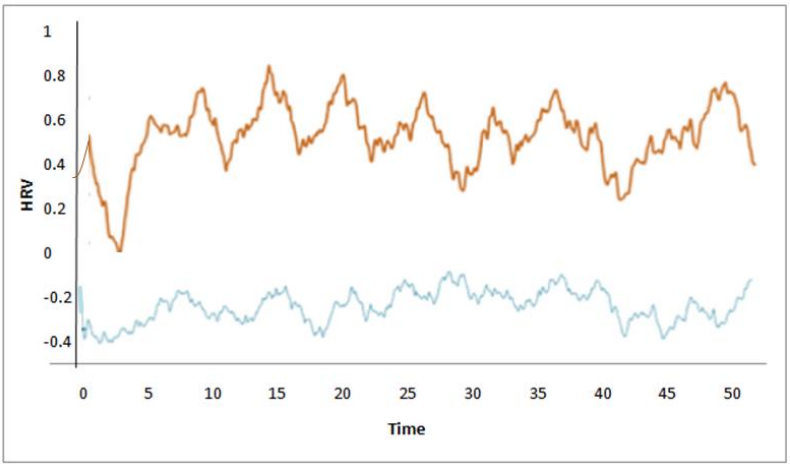

Fig 4: Relationships between HRV elements and Schumann resonances in variations and ULF energy

In the IBIs and HF energy, there was an instantaneous positively linked reaction to variations in ULF energy that lasted 3 hrs.During in the previous two hrs, HF energy became negatively connected. During the first 3 hrs, the LF/HF ratio was adversely associated.

The median ranges of magnitudes & frequencies of the modulating signals were determined and presented in Table 3 based on the findings of AM and FM analyses of the frequency elements retrieved by these 3 techniques from the 3 patient information series. The AM amplitude range grows as the element frequencies fall, however the FM amplitude range falls.Concurrently, AM & FM frequencies are comparable as the actual ranges of frequency range diminish. The synthetic HRV waveform were created using this data in Table 4.

Table 3: The magnitude ranges & frequencies of the AM and FM HRV elements

Variations		High Frequency	Low Frequency	Very Low Frequency	Ultra Low Frequency
Amplitude Modulation	Range (S)	0.2	0.3	0.4	0.5
	Freq (Hertz)	0.02	0.005	0.004	0.003
Frequency Modulation	Range (S)	0.20	0.05	0.02	0.3
	Freq (Hertz)	0.006	0.007	0.004	004

Table 4: Relative errors (δ) and correlation coefficients (r) of components derived using the techniques under consideration

Section	Accuracy					
	MBF		EMD		Short-Time Fourier Transform	
High Frequency	35	0.83	85.2	0.58	83.6	0.6
Low Frequency	17	0.89	42	0.89	62	0.95
Very Low Frequency	14	0.89	32	0.89	126	0.30
Ultra Low Frequency	0.02	2	0.98	0.97	7	0.34

Altogether, this research shows that during periods of typical quiet action, everyday ANS action, as assessed by HRV, responds to fluctuations in magnetism and sunlight action. Moreover, the ANS reactions begin at various periods after alterations in different environmental conditions and last for varying amounts of time. This should be highlighted that various individuals adapt to the new almost the same ecological unit .

IBIs had an inverse connection with pulse rate, with greater IBIs corresponding to a lesser pulse rate. Pulse rate and IBIs are excellent indicators of differences in the overall balancing of parasympathetic and sympathetic action, but rather how the parasympathetic individuals respond to and adjusts to diverse pressures and obstacles [29]. If an environmentelement has a negative relationship with IBIs, it means that as that element increases, pulse rates will rise as well, implying a physiological stress response.

The sunlight radio flow rate indicator was highly related to lowered tiredness, enhanced positive impact, and clarity of mind, whereas rises in sunlight airspeed had the reverse effect. The sunlight flare flow could be a key mediator of predictive responses, which can happen many times before surges in the sunlight flares return To earth and cause magnetic perturbations.Other types of radiation, including X-rays, sunlight radiation, and UV coming from the sun in sunlight flares, are also probably part of the predicted response.

In a big investigation of a young generation with probable inflammatory diseases who already had serum C-reactive protein (CRP) testing done, researchers discovered a strong inverse relationship between C-reactive protein levels and sunlight radiation. Although the exact pathophysiology is unknown, we believe that the energy ambient elements outlined above can change human Psychophysiology and actions in a variety of ways, based on the health history and development of the person [30].

STFT is one of the most widely used methods in this research, owing to its aptitude for computing the energy spectrum of the studied HRV segments. Even though the real time frequencies evaluated for HF, LF, and especially VLF elements were very similar to those from MBF and EMD in terms of simple styles and real time amplitudes, the real time wavelengths evaluated for HF, LF, and especially VLF elements were more and more suppressed with greater frequency (right panel). Simultaneously, it seems that this lower FM evaluation is balanced for by somewhat higher AM orders of magnitude.This could be due to the impact with double average, which was employed to estimate the immediate aspects with the transient spectrum before flattening the regulating tones, therefore an alternative strategy should be considered in the future to resolve this issue. The sliding window breadth, which was originally established equivalent to the long term describing the given frequency range, has a substantial influence on both the STFT results (so compared to MBF and EMD) and the summing impacts.HRV data were processed at 1/2 breadth and multiplied by 2, 3, and 4 to evaluate the influence of window width, but accuracy obtained (in based on the relative error range) did not increase. To conclude, STFT was the least reliable process of extracting biological elements and their attributes from HRV.In two levels, the studied procedures have been statistically appraised. First, three participants' Resp outputs have been matched to the HF elements recovered from HRV, and then the technique's results are evaluated using random numbers, as well as in aspects of the obtained oscillations' resemblance and the simultaneous relative intensities and rates.Thorough assesment of Figure 5 reveals that Resp and HFc morphologies are unrelated, implying that respiration, deep seems to have no serious influence on HRV in the HF region. This result, however, doesn't really apply to the temporal connection of these events. The excellent correlation between both simultaneous stages ($r = 0.93$ for Patients #7 and 11) is a very well association, demonstrating that MBF paired with HT is an effective technique for HRV deconstruction, at least in the HF region.A critical evaluation of studies demonstrate, while Table 2 shows a quantitative comparison. Despite the fact that almost all of the rebuilt components are quite close to the synthetic no stationary waveforms, those retrieved with MBF are the finest and most represent the basic data. The efficacy of MBF, particularly EMD, has even been proven in [31], but the researchers of that publication did not disclose any information regarding the screens employed.MBF's overall gains, which includes every recovered elements along with both indicees – the error percentage of element restoration and also the linear regression r. The results produced here were not clear because current research on HRV adapted to the study of slowly varying data has centered on even more efficient and complex techniques than MBF. The scenario is different when it comes to computation complexity, with EMD has the quickest (0.3 s) and STFT having the longest (1.5 s) (46.7 s).MBF and STFT should use inversion or processing frame, moving all over the information independently for every sought element, despite the fact that EMD is a recurrent technique. In addition, the employed STFT model measures the immediate magnitude and frequency right away.

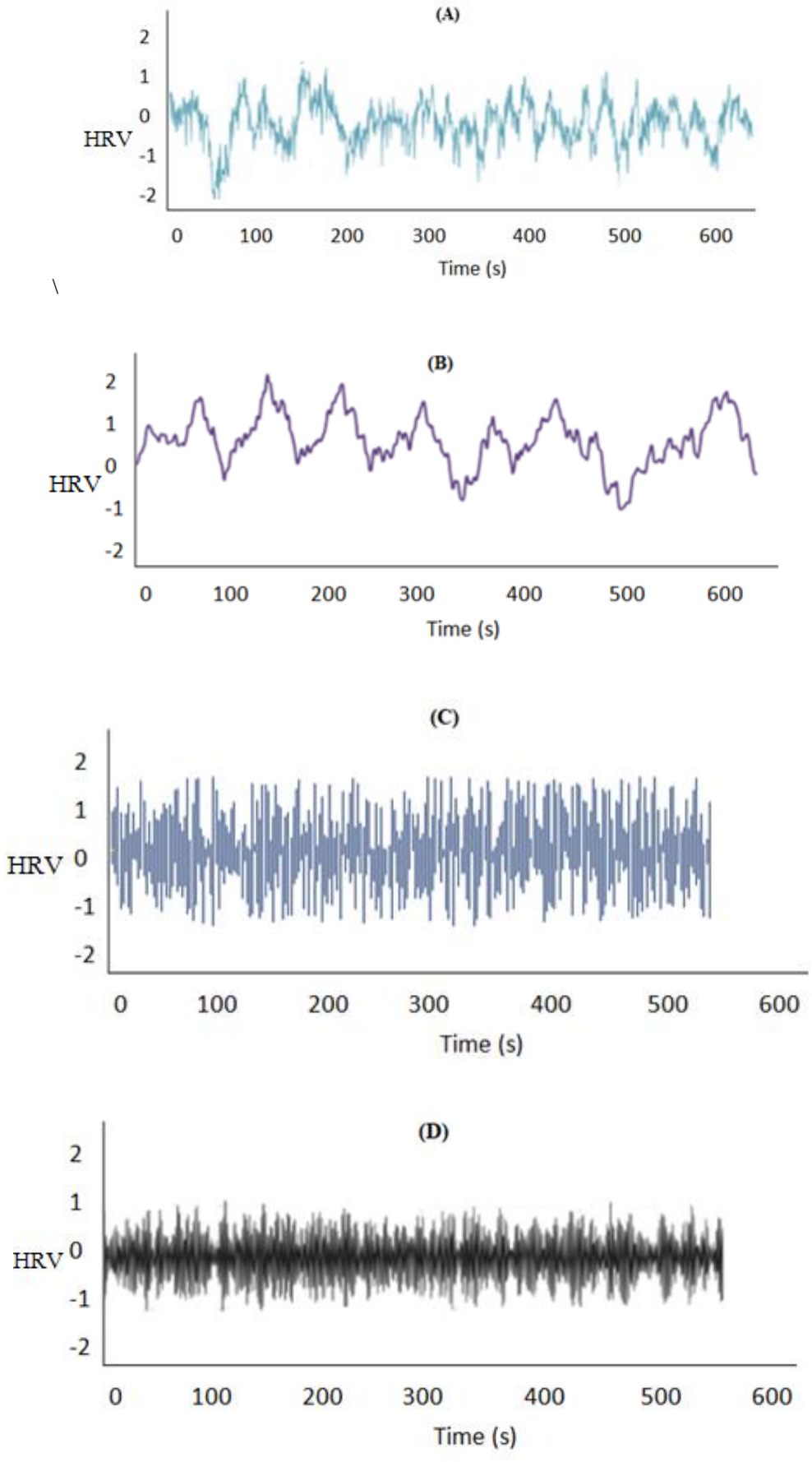

Fig 5: Formalized high frequency components (HFc) collected from three persons' HRVs to use the component techniques: STFT compared to regular pulmonary impulses

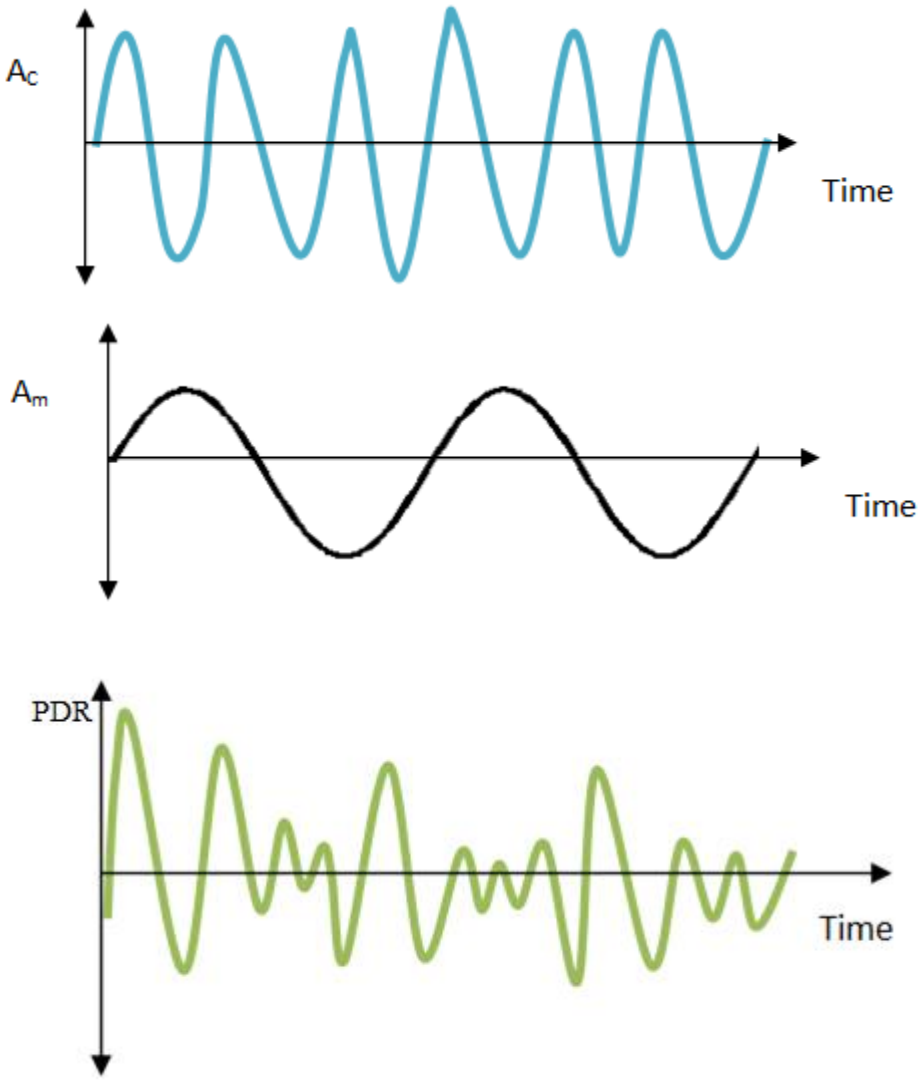

Fig 6: Ac, Am and proposed dynamic range (left panel) and frequency (right panel) recovered with MBF using artificial HRV with their real sequences (blue)

The preceding findings of this research revealed a wealth of knowledge about the biological pathways that control HR as well as the tools that may be utilized to research them. However, there are certain limitations to this approach. One was to look into HRV information with only 3 doses, despite the fact that several data available in Multiple sensor nodes as well as other public databases. This can be explained by concentrating on functional classification for extracting biological elements from HRV rather than the qualities of the biological elements itself, The actual information was mostly required to construct the artificial pulses appropriately. It's also important to emphasize also that recovered elements simply reflect the impact of ANS function on HRV, not really the molecular basis forces. Since previously stated, retrieving the ANS impulses from of the HRV elements is really an important reverse challenge which needs to be resolved and that is not covered in this research.

4.3 UWFR smoothing filter

The aim of the research is to use a UWFR flattening filter to remove the associated noise in ECG data in order to extract characteristics. The aim of the present study is to extract architectural ata from individual ECG signals and analyze them with a normal pace. The significant decrease of sound with an ideal and the adjustable perspective of actual ECG information is a key discovery when using the proposed method. This decrease helps in examining the characteristics of the pulse rate with more accuracy.On the MIT-BIH irregular pules rate set of data, the UWFR softening device to responsive surface outdoes this same sequential predictive model and other UWFR remedies like the UWFR filtration and UWFR forecasting filtration system based on mistakes variations in actual ECG signals and SNRs predicated on ECG artificial provided in multiple estimation techniques. It's worth noting that linear prediction-based techniques for extracting ECG signal characteristics were deemed conventional. In this regard, the improved performance

of the flattening method presented in this study offers up new possibilities for increasing the validity and consistency of diagnosing various types of cardiac illnesses.The efficiency of the UWFR flattening filtering were improved by making the mean boundary adjustment. It's worth noting that easily observed models for ECG signals haven't taken advantage of a chance.

5. Conclusion

Altogether, the research shows how the everyday ANS activity, as measured by HRV, reacts to different through electromagnetic and sunlight energy predominantly at times when sunspot radiance is not disrupted. Moreover, such ANS reactions begin at various periods following alterations in different environmental conditions which last for varying number of hours. Sunlight radiation was found to be negatively related with IBIs, suggesting because when sunlight radiation rises, pulse rate rises, implying a human oxidative stress.Enhanced HRV and enhanced bogus action appear to be linked to enhanced sunlight radiation, sunlight radiation output, and Overall frequency, strength, and the ANS react swiftly to alterations in these environmental elements. Such results back up the theory which those dynamic external elements operate as power sources that manifest in various respects based on an individual especially, mental capacity, and personality ability. Because no single study or piece of data can be regarded conclusive, testimony of chronology is best established when multiple pieces of research point to a certain result. As a result, we examined and recorded various versions of data that carefully evaluated the notion of everyday ANS action, as represented by HRV, reacts to variations in the magneto and sun measured at various intervals and endures over differing time intervals. Furthermore, the data are compatible with and expand on initially disclosed findings. The assessment of variations in distinct induced magnetic surroundings influences the human sympathetic nervous system variably even specifiable adaptive behavior is unique to our research.Even if the data were highly quasi, MBF is somewhat more reliable in the nocturnal HRV routine assessment than the other 2 tested systems, namely EMD and STFT. It's achievable because the UWFR flattening tube's sequence and ordinary vista have been adjusted in such a way that the vista is becoming responsive to separate parts of ECG waveform.

References

[1] Syed Zafar SN, Umar R, Sabri NH, Jusoh MH, Dagang AN, Yoshikawa A. Effects of solar flares and coronal mass ejections on Earth's horizontal magnetic field and solar wind parameters during the minimum solar cycle 24. Monthly Notices of the Royal Astronomical Society. 2021 Jul;504(3):3812-22.

[2] Kappenman J, Radasky W. Geomagnetic Field Impacts on Ground Systems. Space Weather Effects and Applications. 2021 Mar 19:183-213.

[3] Mandea M, Chambodut A. Geomagnetic field processes and their implications for space weather. Surveys in Geophysics. 2020 Nov;41(6):1611-27.

[4] Simi KG, Akala AO, Krishna KS, Amaechi PO, Ogwala A, Ratnam DV, Oyedokun OJ. Responses of the Indian Equatorial Ionization Anomaly to two CME-induced geomagnetic storms during the peak phase of solar cycle 24. Advances in Space Research. 2021 Jun 15.

[5] Ponomarev A, Tyapochkin K, Surkova E, Smorodnikova E, Pravdin P. Heart Rate Variability as a Prospective Predictor of Early COVID-19 Symptoms. medRxiv. 2021 Jan 1.

[6] Christodoulou G, Salami N, Black DS. The utility of heart rate variability in mindfulness research. Mindfulness. 2020 Mar;11(3):554-70.

[7] Schuurmans AA, de Looff P, Nijhof KS, Rosada C, Scholte RH, Popma A, Otten R. Validity of the Empatica E4 wristband to measure heart rate variability (HRV) parameters: A comparison to electrocardiography (ECG). Journal of medical systems. 2020 Nov;44(11):1-1.

[8] Taylor DL, Grant DM, Kraft JD, Frosio KE, White EJ, Judah MR, Mills AC. The role of parasympathetic activity in the relationship between worry and neural indicators of attentional control. Psychology & Neuroscience. 2020 Mar;13(1):51.

[9] Dyavanapalli J. Novel approaches to restore parasympathetic activity to the heart in cardiorespiratory diseases. American Journal of Physiology-Heart and Circulatory Physiology. 2020 Dec 1;319(6):H1153-61.

[10] Jauniaux J, Tessier MH, Regueiro S, Chouchou F, Fortin-Côté A, Jackson PL. Emotion regulation of others' positive and negative emotions is related to distinct patterns of heart rate variability and situational empathy. PloS one. 2020 Dec 31;15(12):e0244427.

[11] McCraty R, Atkinson M, Dispenza J. One-Minute Deep Breathing Assessment and its Relationship to 24-Hour HRV Measurements. Biofeedback. 2021;49(2):27-37.

[12] Shi Y, Jiang R, Zhu C, Zhang M, Cai H, Hu Z, Ye Y, Liu Y, Sun H, Ma Y, Cao X. High Job Burnout Predicts Low Heart Rate Variability in the Working Population after a First Episode of Acute Coronary Syndrome. International Journal of Environmental Research and Public Health. 2021 Jan;18(7):3431.

[13] Huang C, Tang M, Li H, Wen J, Wang C, Gao Y, Hu J, Lin J, Chen R. Particulate matter air pollution and reduced heart rate variability: How the associations vary by particle size in Shanghai, China. Ecotoxicology and Environmental Safety. 2021 Jan 15;208:111726.

[14] Li L, Li H, He L, Chen H, Li Y. Study on the Relationship Between Orthostatic Hypotension and Heart Rate Variability, Pulse Wave Velocity Index, and Frailty Index in the Elderly: A Retrospective Observational Study. Frontiers in cardiovascular medicine. 2020;7.

[15] Lu T, Chen YF, Hechtman B, Wang T, Anderson J. Large-scale discrete Fourier transform on TPUs. IEEE Access. 2021 Jun 25;9:93422-32.

[16] Chui CK, Jiang Q, Li L, Lu J. Analysis of an adaptive short-time Fourier transform-based multicomponent signal separation method derived from linear chirp local approximation. Journal of Computational and Applied Mathematics. 2021 Nov 1;396:113607.

[17] Meignen S, Colominas M, Pham DH. On the use of rényi entropy for optimal window size computation in the short-time fourier transform. InICASSP 2020-2020 IEEE International Conference on Acoustics, Speech and Signal Processing (ICASSP) 2020 May 4 (pp. 5830-5834). IEEE.

[18] Iftode IA, Fosalau C. Wavelet-based Techniques Applied to Digital Processing of ECG Signals. In2020 International Conference and Exposition on Electrical And Power Engineering (EPE) 2020 Oct 22 (pp. 419-424). IEEE.

[19] Celeste V, Corbet S, Gurdgiev C. Fractal dynamics and wavelet analysis: Deep volatility and return properties of Bitcoin, Ethereum and Ripple. The Quarterly Review of Economics and Finance. 2020 May 1;76:310-24.

[20] Christifano DN, Taylor MK, Carlson SE, Colombo J, Gustafson KM. Higher maternal weight is related to poorer fetal autonomic function. Journal of Developmental Origins of Health and Disease. 2021 Jun;12(3):354-6.

[21] Satheeskumaran S, Venkatesan C, Saravanan S. Real-time ECG signal pre-processing and neuro fuzzy-based CHD risk prediction. International Journal of Computational Science and Engineering. 2021;24(4):323-30.

[22] Vargas-Lopez O, Amezquita-Sanchez JP, De-Santiago-Perez JJ, Rivera-Guillen JR, Valtierra-Rodriguez M, Toledano-Ayala M, Perez-Ramirez CA. A new methodology based on EMD and nonlinear measurements for sudden cardiac death detection. Sensors. 2020 Jan;20(1):9.

[23] Satheeskumaran S, Venkatesan C, Saravanan S. Real-time ECG signal pre-processing and neuro fuzzy-based CHD risk prediction. International Journal of Computational Science and Engineering. 2021;24(4):323-30.

[24] Pei Z, Shi M, Guo J, Shen B. Heart rate variability based prediction of personalized drug therapeutic response: the present status and the perspectives. Current Topics in Medicinal Chemistry. 2020 Jul 1;20(18):1640-50.

[25] Ilan Y. Establishment of an Individualized Chronotherapy, Autonomic Nervous System, and Variability-Based Dynamic Platform for Overcoming the Loss of Response to Analgesics. Pain Physician. 2021 May;24:243-52.

[26] Mejía-Mejía E, Budidha K, Abay TY, May JM, Kyriacou PA. Heart rate variability (HRV) and pulse rate variability (PRV) for the assessment of autonomic responses. Frontiers in physiology. 2020 Jul 23;11:779.

[27] Gao N, Marschall M, Burry J, Watkins S, Salim FD. Understanding occupants' behaviour, engagement, emotion, and comfort indoors with heterogeneous sensors and wearables. arXiv preprint arXiv:2105.06637. 2021 May 14.

[28] Djurhuus A, Closek CJ, Kelly RP, Pitz KJ, Michisaki RP, Starks HA, Walz KR, Andruszkiewicz EA, Olesin E, Hubbard K, Montes E. Environmental DNA reveals seasonal shifts and potential interactions in a marine community. Nature communications. 2020 Jan 14;11(1):1-9.

[29] Gowayed MA, Mahmoud SA, Michel TN, Kamel MA, El-Tahan RA. Galantamine in rheumatoid arthritis: A cross talk of parasympathetic and sympathetic system regulates synovium-derived microRNAs and related pathogenic pathways. European Journal of Pharmacology. 2020 Sep 15;883:173315.

[30] Alabdulgader AA. Space and Human Consciousness: The Great Whisper. Natural Science. 2021 Jul 8;13(7):235-53.

[31] Wenning C, Vrachimis A, Pavenstädt HJ, Reuter S, Schäfers M. Coronary artery calcium burden, carotid atherosclerotic plaque burden, and myocardial blood flow in patients with end-stage renal disease: A non-invasive imaging study combining PET/CT and 3D ultrasound. Journal of Nuclear Cardiology. 2020 Mar 5:1-1.